

Methylation-Associated Silencing of the *Nuclear Receptor 112* Gene in Advanced-Type Neuroblastomas, Identified by Bacterial Artificial Chromosome Array-Based Methylated CpG Island Amplification

Akiko Misawa,^{1,4} Jun Inoue,^{1,4} Yuriko Sugino,^{1,4,5} Hajime Hosoi,⁵ Tohru Sugimoto,⁵ Fumie Hosoda,³ Misao Ohki,³ Issei Imoto,^{1,4} and Johji Inazawa^{1,2,4}

¹Department of Molecular Cytogenetics, Medical Research Institute and Graduate School of Biomedical Science and ²Center of Excellence Program for Frontier Research on Molecular Destruction and Reconstitution of Tooth and Bone, Tokyo Medical and Dental University; ³Cancer Genomics Project, National Cancer Center Research Institute, Tokyo, Japan; ⁴Core Research for Evolutionary Science and Technology of the Japan Science and Technology Corporation, Saitama, Japan; and ⁵Department of Pediatrics, Kyoto Prefectural University of Medicine, Kyoto, Japan

Abstract

To identify genes whose expression patterns are altered by methylation of DNA, we established a method for scanning human genomes for methylated DNA sequences, namely bacterial artificial chromosome array-based methylated CpG island amplification (BAMCA). In the course of a program using BAMCA to screen neuroblastoma cell lines for aberrant DNA methylation compared with stage I primary neuroblastoma tumors, we identified CpG methylation-dependent silencing of the *nuclear receptor 112* (*NR112*) gene. *NR112* was methylated in a subset of neuroblastoma cell lines and also in advanced-stage primary tumors with amplification of *MYCN*. Its methylation status was inversely associated with gene expression. Treatment with the demethylating agent 5-aza-2'-deoxycytidine restored *NR112* transcription in neuroblastoma cell lines lacking endogenous expression of this gene. A CpG island located around exon 3 of *NR112* showed promoter activity, and its methylation status was clearly and inversely correlated with *NR112* expression status. The gene product, NR112, has a known function in regulating response to xenobiotic agents but it also suppressed growth of neuroblastoma cells in our experiments. We identified some possible transcriptional targets of NR112 by expression array analysis. The high prevalence of *NR112* silencing by methylation in aggressive neuroblastomas, together with the growth-suppressive activity of NR112, suggests that this molecule could serve as a diagnostic marker to predict prognosis for neuroblastomas. (Cancer Res 2005; 65(22): 10233-42)

Introduction

Neuroblastoma, the most common extracranial solid tumor of childhood, has distinct biological characteristics in different pro-

gnostic subgroups. Children (>12 months at diagnosis) with stage IV or *MYCN*-amplified stage III tumors are at high risk of mortality (>60%), children with non-*MYCN*-amplified local-regional tumors (i.e., stages I, II, and III) and infants (<12 months at diagnosis) with stage IVS disease are generally at low risk of mortality (<10%), and infants with stage IV disease and children with stage III disease without *MYCN* amplification are at intermediate risk (1, 2), although the biological basis for that clinical diversity remains unclear. In addition to genetic changes including the *MYCN* amplification, epigenetic alterations often play important roles in the pathogenesis of human cancers, including neuroblastoma (3). For example, hypermethylation of promoter sequences of *CASP8*, *RASSF1A*, *CD44*, *TSP-1*, and *HSP47* genes has been observed in neuroblastoma tumors (4–8), and silencing of *CASP8* through methylation of its promoter tends to be associated with *MYCN* amplification (4). A reported positive correlation between promoter hypermethylation of *CASP8* and *RASSF1A* (5) suggests that hypermethylation of multiple genes may influence the phenotype of neuroblastoma.

Because hypermethylation in CpG-rich promoter or exonic regions seems to be a critical contributor to inactivation of tumor suppressor genes in many human cancers through transcriptional silencing (9), identification of hypermethylated CpG-rich sequence in cancer cell genomes could accelerate identification of unknown tumor suppressors. Although several techniques, including a method known as methylated CpG island amplification (MCA), have been developed (10, 11), we still have limited number of effective and practical high-throughput methods for genome-wide screening of aberrantly methylated CpG-rich sequences. To accomplish high-throughput screening for methylated sites in the entire genome, we developed a bacterial artificial chromosome (BAC) array-based MCA (BAMCA), incorporating our custom-made, BAC-based genomic DNA array combined with MCA (12).

In an effort to identify genes that are silenced by methylation mechanisms and associated with progression of neuroblastoma, we applied BAMCA to human neuroblastoma in the study reported here. Because the pattern of genomic changes observed in most neuroblastoma-derived cell lines is similar to that of advanced primary neuroblastomas (13), we used DNAs from neuroblastoma cell lines and from stage I primary tumors as test and reference samples, respectively. Using this approach, we successfully identified one gene, *nuclear receptor 112* (*NR112*), also known as *PXR*, whose expression was decreased in a subset of

Note: A. Misawa and J. Inoue contributed equally to this work.

Supplementary data for this article are available at Cancer Research Online (<http://cancerres.aacrjournals.org/>).

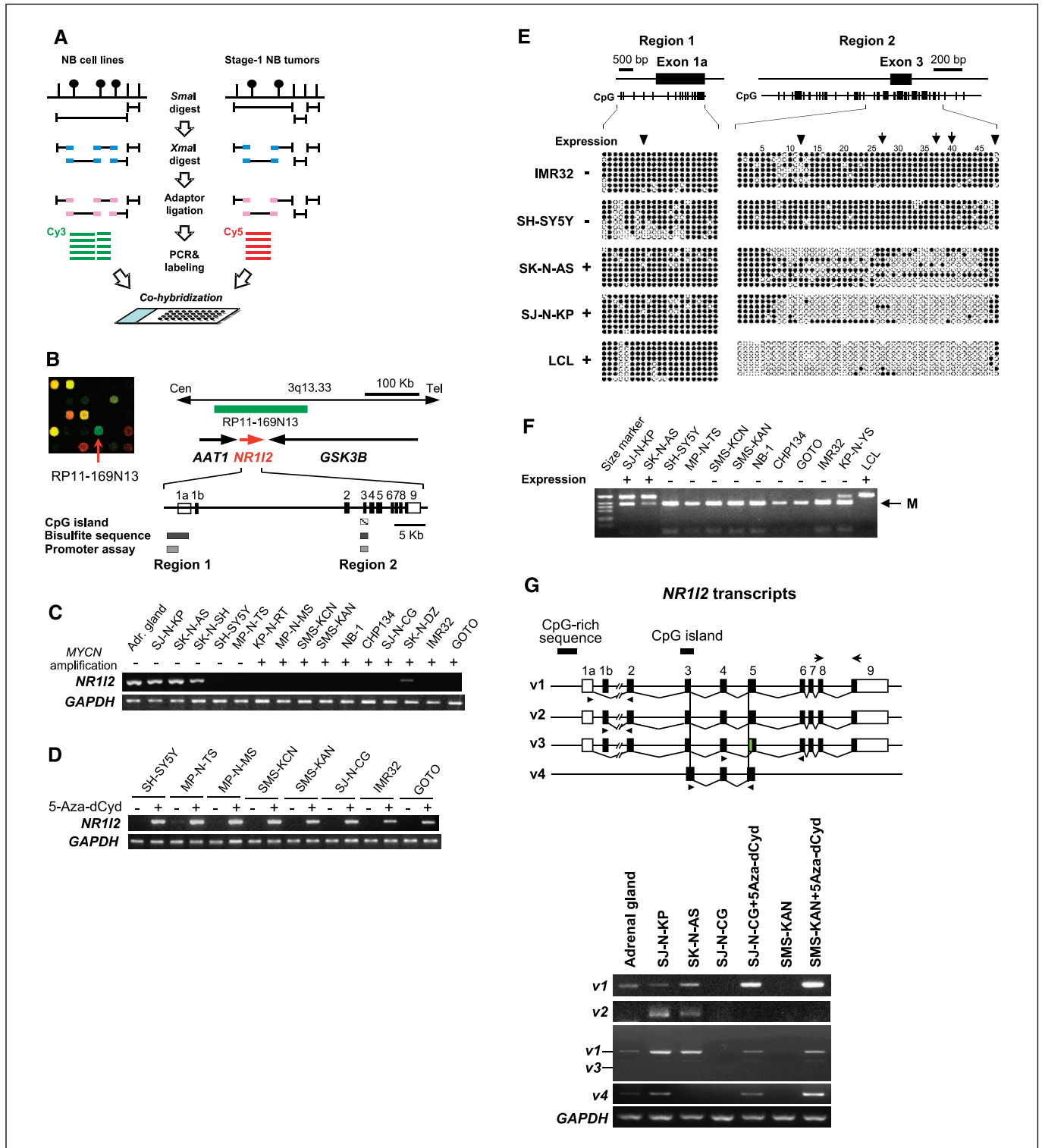
Requests for reprints: Johji Inazawa, Department of Molecular Cytogenetics, Medical Research Institute, Tokyo Medical and Dental University, 1-5-45 Yushima, Bunkyo-ku, 113-8510 Tokyo, Japan. Phone: 81-3-5803-5820; Fax: 81-3-5803-0244; E-mail: johinaz.cgen@mri.tmd.ac.jp.

©2005 American Association for Cancer Research.
doi:10.1158/0008-5472.CAN-05-1073

human cell lines and tumors of neuroblastoma through hypermethylation of a CpG island showing promoter activity. *NR112* was methylated and silenced mainly in late-stage neuroblastoma tumors with *MYCN* amplification and in older children. Exogenous restoration of *NR112* expression suppressed growth of neuroblastoma cells lacking endogenous expression of the gene.

Materials and Methods

Cell culture, drug treatment, and primary tissue samples. All 19 human neuroblastoma cell lines we used (SK-N-KS, SK-N-AS, SK-N-SH, SK-N-DZ, SH-SY5Y, MP-N-TS, MP-N-MS, KP-N-RT, KP-N-SIFA, KP-N-SILA, KP-N-TK, KP-N-YS, SMS-KCN, SMS-KAN, SJ-N-CG, NB-1, CHP134, IMR32, and GOTO) had been established from surgically resected tumors and maintained as described previously (13). These cultures



were treated with or without 1 $\mu\text{mol/L}$ 5-aza 2'-deoxycytidine (5-aza-dCyd) for 5 days.

Primary tumor samples were obtained at surgery from 51 neuroblastoma patients who underwent tumor resection at University Hospital, Kyoto Prefectural University of Medicine from 1986 to 2003, with written consent from the parents of each patient in the formal style and after approval by the local ethics committees. Staging was evaluated according to the criteria of the International Neuroblastoma Staging System (14). Of the 51 cases, 12 were classified as stage I, 11 as stage II, eight as stage III, 13 as stage IV, and four as stage IVS. Thirty-seven of the patients were infants <1 year of age at diagnosis. *MYCN* amplification was detected in 8 of 51 cases (15%). In 39 cases (76%), neuroblastoma had been detected by a mass screening program. Patients were treated according to previously described protocols (15, 16). Tumor samples were frozen immediately and stored at -80°C until required.

Bacterial artificial chromosome array-based methylated CpG island amplification. The preparation of DNA probes for screening of methylated regions was carried out by the MCA method described by Toyota et al. (11). Five-microgram aliquots of test DNA were first digested with 100 units of a methylation-sensitive restriction enzyme *SmaI* and subsequently with 20 units of methylation-insensitive *XmaI*. Adaptors were ligated to *XmaI*-digested sticky ends and PCRs were done with an adaptor primer and Cy3-dCTP for labeling. Control DNA was treated in the same manner except that labeling was with Cy5-dCTP (Fig. 1A).

Labeled test and control PCR products were cohybridized to our in-house array (MCG Whole Genome Array-4500; ref. 12). Hybridizations were carried out as described elsewhere (17). Arrays were scanned with a GenePix 4000B (Axon Instruments, Foster City, CA) and analyzed using GenePix Pro 4.1 software (Axon Instruments).

Reverse transcription-PCR and real-time quantitative reverse transcription-PCR. Single-stranded cDNAs were generated from total RNAs (17) and amplified with specific primers for each gene. Primer sequences are available on request. Real-time quantitative PCR was done using LightCycler (Roche Diagnostics, Tokyo, Japan) with SYBR green as described previously (18). The *glyceraldehyde-3-phosphate dehydrogenase* (*GAPDH*) gene served as an endogenous control. Each sample was normalized on the basis of its *GAPDH* content. PCR amplification was done in duplicate for each sample.

Methylation analysis. To investigate methylation of DNA, the method of combined bisulfite restriction analysis (COBRA) was done as described earlier (11). Genomic DNAs were treated with sodium bisulfite and subjected to PCR using primer sets designed to amplify the regions of interest. PCR products were digested with *HhaI*, which recognizes sequences unique to the methylated alleles but cannot recognize unmethylated alleles, and electrophoresed. For bisulfite sequencing, PCR products were subcloned and sequenced.

Reporter assay. A 1,060 bp fragment upstream of exon 1 of *NR112* (region 1; Fig. 1A) and a 480 bp fragment of a CpG island that includes exon

3 (region 2; Fig. 1A) were ligated into the pGL3-Basic vector (Promega, Madison, WI) in front of and/or downstream of the luciferase gene. An equal amount of each construct was introduced into cells with an internal control vector (pRL-hTK, Promega), using FuGENE 6 (Roche Diagnostics). A pGL3-Basic vector without insert served as a negative control. Firefly luciferase and *Renilla* luciferase activities were each measured 36 hours after transfection using the Dual-Luciferase Reporter Assay System (Promega); relative luciferase activities were calculated and normalized versus *Renilla* luciferase activity.

Transfection, Western blotting, and colony formation assays. A full-length *NR112* cDNA was cloned into the pCMV-Tag3 eukaryotic expression vector (Stratagene, La Jolla, CA) with or without epitope (VP-16) in-frame along with the Myc epitope. A plasmid expressing a Myc-tagged *NR112* with or without VP-16 (pCMV-Tag3-VP-*NR112* or pCMV-Tag3-*NR112*), or the empty vector (pCMV-Tag3-mock), were transfected into cells using FuGENE6 (Roche Diagnostics). Expression of *NR112* protein in transfected cells was confirmed by Western blotting using anti-Myc-Tag antibody (9B11; Cell Signaling Technology, Beverly, MA). For colony formation assays, transfected cells were selected with 500 $\mu\text{g/mL}$ G418; 3 weeks after transfection, the neomycin-resistant colonies were stained with crystal violet and counted (17).

Cell growth assay. Stable *NR112* transfectants and controls were obtained by transfecting pCMV-Tag3-VP-*NR112* or pCMV-Tag3-mock, respectively, into cells lacking *NR112* expression. For measurements of cell growth, 2×10^3 cells were seeded in 96-well plates. The numbers of viable cells were assessed by a colorimetric water-soluble tetrazolium salt assay (cell counting kit-8; Dojindo Laboratories, Kumamoto, Japan).

Oligonucleotide array analysis. mRNA expression profiling was done using the AceGene Human oligo chip 30K (DNA Chip Research, Inc., Kanagawa, Japan), containing 30,000 genes, as described elsewhere (18). The test and reference cDNA probes labeled with aminoallyl-dUTP (Ambion, Inc., Austin, TX) were synthesized using oligo(dT)12-18 primer and coupled with Cy3- or Cy5-monoreactive dye (Amersham Biosciences, Tokyo, Japan), respectively. The hybridized chips were scanned using GenePix 4000B (Axon Instruments) and analyzed using GenePix Pro 4.1 software (Axon Instruments). Signal intensities between the two fluorescent images were normalized by the averaged values for blank spots; this procedure effectively defined the signal intensity-weighted spot for the internal controls of housekeeping genes on each array to have a Cy3/Cy5 ratio of 1.0.

Results

Methylation analysis of neuroblastoma cell lines by bacterial artificial chromosome array-based methylated CpG island amplification. To assess DNA methylation in the more advanced type of neuroblastoma tumors, we did BAMCA

Figure 1. Methylation status and expression levels of *NR112* in neuroblastoma (*NB*) cell lines. **A**, BAMCA procedure. The DNAs from neuroblastoma cell lines (test) or stage I neuroblastoma tumors (control) were first digested with *SmaI* in the blunt end and subsequently with *XmaI* in the sticky end (blue boxes). Adaptors were ligated to *XmaI*-digested sticky ends (pink boxes) and PCR was done with an adaptor primer and Cy3-dCTP (test) or Cy5-dCTP (control) for labeling. Labeled PCR products were cohybridized to BAC array. **B**, left, representative image of BAMCA analysis applied to the IMR32 cell line. Green, BAC containing highly methylated fragments in IMR32 compared with stage I tumors; red, BAC containing highly methylated fragments in stage I tumors compared with IMR32; yellow, unchanged methylation status; black, no detectable methylated fragments. The RP11-169N13 BAC (arrow) harboring *NR112* was detected as spot with a high Cy3 (test)/Cy5 (control) ratio. Right, genomic structure of the *NR112* gene consisting of nine exons. A 239 bp CpG island exists around exon 3 (Genbank accession nos. NM_003889 for cDNA sequence and NT_005612 for genomic sequence). Horizontal bars, regions examined in a promoter assay and bisulfite sequencing analysis (regions 1 and 2). **C**, representative results of RT-PCR analysis of *NR112* mRNA expression in normal adrenal gland and neuroblastoma cell lines with (+) or without (-) amplification of *MYCN*. *GAPDH* was used as an internal control. **D**, representative results of RT-PCR analysis to reveal *NR112* expression in neuroblastoma cell lines with (+) and without (-) treatment with 5-aza-dCyd. *GAPDH* was used as an internal control. **E**, top, map of the 5' region (exon 1 and upstream sequence, region 1) and the CpG island around exon 3 (region 2) in *NR112*. Vertical tick marks, CpG sites. Bottom, results of bisulfite sequencing analysis done in *NR112*-nonexpressing cell lines (IMR32 and SH-SY5Y) and *NR112*-expressing cell lines (SK-N-AS, SJ-N-KP, and LCL). \circ , unmethylated CpG sites; \bullet , methylated CpG sites, respectively; each row represents a single clone. Arrows, *HhaI* restriction site. Arrowheads, *SmaI* restriction site. **F**, representative results of COBRA of region 2 in neuroblastoma cell lines with (+) or without (-) *NR112* expression. A 492 bp PCR product, including exon 3, was restricted by *HhaI*. **M**, methylated alleles. **G**, top, map of four variants (*v1-v4*) and location of each primer set used for RT-PCR analysis. Black boxes, coding exons; gray box, deleted region in variant 3. Arrows, primers used for RT-PCR shown in (B and C), and in Fig. 2B and C; arrowheads, primer sets specific for each variant. Nucleotide sequences for primers used are available on request. Bottom, representative results of RT-PCR analysis. A primer set for variant 3 amplified two products with 441 and 330 bp sizes from variants 1 and 3, respectively.

Table 1. List of positive BACs in BAMCA analysis and summary of screening of candidate methylated genes

	BAC (RP11)	Locus	Gene		CpG island*
			Symbol	Name	
1	73D7	<i>1q32.1</i>	<i>LHX9</i>	<i>LIM homeobox 9</i>	+
2	451A14	<i>2p24</i>	No gene		
3	169N13	<i>3q13.3</i>	<i>NRII2</i>	<i>Nuclear receptor subfamily 1, 2group 1, member 2</i>	+
			<i>GSK3B</i>	<i>Glycogen synthase kinase 3β</i>	—
			<i>AAT1</i>	<i>AAT1-α</i>	—
4	205N12	<i>4p15.1</i>	<i>PCDH7</i>	<i>Protocadherin 7</i>	+
5	17P19	<i>4q21.2</i>	<i>MRPL1</i>	<i>Mitochondrial ribosomal protein L1</i>	—
6	611D20	<i>9q34</i>	<i>NOTCH1</i>	<i>Notch homologue 1, translocation-associated (Drosophila)</i>	+
7	248C1	<i>10q23.33</i>	<i>MPHOSPH1</i>	<i>M-phase phosphoprotein 1</i>	+
8	37L21	<i>10q24</i>	<i>SEMA4G</i>	<i>Sema domain, immunoglobulin domain, transmembrane domain and short cytoplasmic domain (semaphorin) 4G</i>	+
			<i>MRPL43</i>	<i>Mitochondrial ribosomal protein L43</i>	+
9	23E5	<i>11p15.1</i>	<i>DELGEF</i>	<i>Deafness locus associated putative guanine nucleotide exchange factor</i>	+
10	56E13	<i>11p11.2</i>	<i>PTPRJ</i>	<i>Protein tyrosine phosphatase, receptor type, J</i>	+
11	79L5	<i>18q21.2</i>	<i>ONECUT2</i>	<i>One cut domain, family member 2</i>	+
12	7F10	<i>20p11.22</i>	<i>PAX1</i>	<i>Paired box gene 1</i>	+
13	124D1	<i>20q13</i>	<i>PREX1</i>	<i>Phosphatidylinositol 3,4,5-trisphosphate-dependent RAC exchanger 1</i>	+
14	93B14	<i>20q13.33</i>	<i>FLJ32154</i>	unknown	+
			<i>SLCO4A1</i>	<i>Solute carrier organic anion transporter family, member 4A1</i>	+
			<i>NTSR1</i>	<i>Neurotensin receptor 1 (high affinity)</i>	+
15	58O1	<i>10q22.1</i>	<i>SLC29A3</i>	<i>Solute carrier family 29 (nucleoside transporters), member 3</i>	+
			<i>UNC5B</i>	<i>Unc-5 homologue B (Caenorhabditis elegans)</i>	+
16	88B12	<i>10q26.2</i>	<i>MGC32871</i>	<i>Hypothetical protein</i>	—
			<i>PTPRE</i>	<i>Protein tyrosine phosphatase, receptor type, E</i>	+
17	262M8	<i>14q21.3</i>	<i>PTGDR</i>	<i>Prostaglandin D2 receptor</i>	+
			<i>PTGER2</i>	<i>Prostaglandin E receptor 2 (subtype EP2), 53 kDa</i>	+
18	79J21	<i>15q24</i>	<i>ETFA</i>	<i>Electron-transfer-flavoprotein, apolypeptide (glutaric aciduria II)</i>	—
			<i>ISL2</i>	<i>ISL2 transcription factor, LIM/homeodomain, (islet-2)</i>	+

*CpG islands were searched using NCBI human genome database (<http://www.ncbi.nlm.nih.gov/>).

†Each Cy3-labeled neuroblastoma cell line sample/Cy5-labeled mixed stage I neuroblastoma tumor samples (see Fig. 1A).

‡Methylation status in primary tumors was determined by using bisulfite-PCR analysis (see Fig. 2A). —, ≤5%; ±, >5% and ≤50%; +, >50%.

§GOTO cells were treated with 1 μmol/L of 5-aza-dCyd for 5 days (see Fig. 1C).

(Fig. 1A) with our MCG Whole Genome Array-4500 (12) using DNA from each of two neuroblastoma cell lines (IMR32 and GOTO) and mixed DNA from five stage I primary neuroblastoma tumors as test and control DNAs, respectively. As shown in Table 1, 18 BACs, which contain 24 known genes and two uncharacterized transcripts, showed high Cy3 (test)/Cy5 (control) ratios (>1.5) by BAMCA in both cell lines, and were selected as sequences whose CpG sites were frequently methylated in advanced types of neuroblastoma tumors. The same result was obtained in the repeated experiments using the same samples (data not shown), suggesting that BAMCA is a reproducible method. We then selected possible candidates by sequentially analyzing the following: (a) the expression status of each gene in stage I primary neuroblastoma tumors and in IMR32 and GOTO cells; (b) restoration of gene expression after treatment with 5-aza-dCyd; and (c) methylation status of CpG islands around each candidate gene in stage I and stage IVa primary neuroblastoma tumors (data not shown). As shown in Table 1, *NRII2* located within RP11-169N13 (Fig. 1B) emerged as a gene that was (a) expressed in stage I tumors but not in the two neuroblastoma cell lines, (b) restored after treatment with

5-aza-dCyd, and (c) frequently methylated in stage IVa tumors but infrequently in stage I tumors. Those results prompted us to perform detailed analysis of the *NRII2* gene as a putative tumor suppressor whose silencing by a DNA methylation mechanism might be associated with progression of neuroblastoma.

Analysis of *NRII2* expression in neuroblastoma cell lines.

When we examined *NRII2* expression in our panel of 19 neuroblastoma cell lines by reverse transcription-PCR (RT-PCR; Fig. 1C), no *NRII2* mRNA was detected in 14 of the lines (73%): in 11 of 12 *MYCN* amplified lines (91%) or in 3 of 7 *MYCN* nonamplified lines (43%). One line, MP-N-TS, lacking expression of *NRII2* and without *MYCN* amplification, does show *c-MYC* amplification (13). Normal adrenal gland, which is considered the tissue of origin for neuroblastoma tumors, expressed *NRII2* mRNA.

To investigate whether demethylation could restore *NRII2* mRNA in neuroblastoma cells lacking endogenous expression, we treated cells with 1 μmol/L of 5-aza-dCyd, a methyltransferase inhibitor, for 5 days. Expression of *NRII2* mRNA was remarkably increased after the treatment (Fig. 1D).

Table 1. List of positive BACs in BAMCA analysis and summary of screening of candidate methylated genes (Cont'd)

BAMCA ratio [†]		mRNA expression				Methylation [‡]	
GOTO	IMR32	Stage I	IMR32	GOTO	GOTO (+5-aza-dCyd) [§]	Stage I	Stage IVa
3.46	4.57	—	+	+			
1.91	10.78						
1.68	2.10	+	—	—	+	—	+
		+	+	+			
		+	+	+			
3.01	5.19	+	+	+			
2.10	2.05	+	+	+			
1.72	2.33	+	+	+			
3.07	5.54	+	+	+			
2.54	2.32	+	+				
		+	+	+			
3.52	2.17	+	—	+			
3.31	2.48	+	—	—	—		
3.89	5.45	+	+	+			
3.72	12.90	+	—	+			
2.06	1.45	+	+	+			
2.51	3.51	—	—	—			
		+	+	+			
		+	+	—			
1.81	1.85	+	+	+			
		+	+	+			
1.75	16.90	+	—	—	—	—	±
		+	—	—	±	—	±
2.93	3.24	+	—	—	+	—	±
		+	—	—	+	—	±
1.54	3.39	+	+	+			
		—	+	+			

Methylation of NR112 CpG island in neuroblastoma cell lines. We next examined the methylation status of the slightly CpG-rich 5' region (region 1) and the CpG island including exon 3 (region 2) of the NR112 gene, which had been detected by the National Center for Biotechnology Information (NCBI) human genome database⁶ as shown in Fig. 1E. Bisulfite sequencing analysis of region 2 revealed aberrant DNA hypermethylation in IMR32 and SH-SY5Y cell lines lacking expression of NR112, but hypomethylation in two lines expressing the gene (SK-N-AS and SK-N-KP) and in a normal lymphoblast cell line (LCL). On the other hand, no significant difference in methylation pattern within region 1 was observed among those four neuroblastoma cell lines and LCL, regardless of expression status. We did COBRA to confirm the relationship between expression and methylation status within region 2 in a larger set of neuroblastoma cell lines. Predominant methylated alleles were detected in all lines lacking NR112 expression (Fig. 1F and data not shown).

Because several splicing variants of NR112, including the variant starting transcription from exon 3 (variant 4, v4), have been reported in various human tissues (19),⁷ we did RT-PCR using

specific primers for each variant to examine which transcripts might be silenced through a DNA methylation within region 2 in neuroblastoma cell lines (Fig. 1G). Variant 1, the most major variant in various human tissues, and variant 2 were expressed in unmethylated neuroblastoma cell lines, but not in methylated lines, whereas variant 4 without open reading frame was not expressed in one of the unmethylated cell lines (SK-N-AS). The expression of variant 1 and variant 4 was restored after the treatment with 5-aza-dCyd in methylated neuroblastoma cell lines, whereas the expression of variant 2 was not. Variant 3, lacking a part of exon 5, was not expressed in neuroblastoma cell lines regardless of methylation status within CpG island and 5-aza-dCyd treatment. Those results suggested that the methylation of CpG residues in region 2 might be mainly responsible for the silencing of variant 1 of the NR112 gene starting transcription from exon 1a in neuroblastoma, although region 2 does not contain its transcriptional start site.

Promoter activity of the CpG island located around exon 3 of NR112. Because the CpG island (region 2) of NR112 was located around exon 3, we first determined whether region 2 had promoter activity by means of a luciferase reporter assay. This fragment alone (Fig. 2A, 2/L) revealed clear promoter activity, whereas region 1 fragment upstream of exon 1 (Fig. 2A, 1/L) showed almost none (Fig. 2B). In addition, we next determined whether region 2 acts as an enhancer to stimulate transcription from exon 1 by testing the luciferase activity in construct

⁶ <http://www.ncbi.nlm.nih.gov/>.

⁷ <http://www.ncbi.nlm.nih.gov/IEB/Research/Acembly/index.html>.

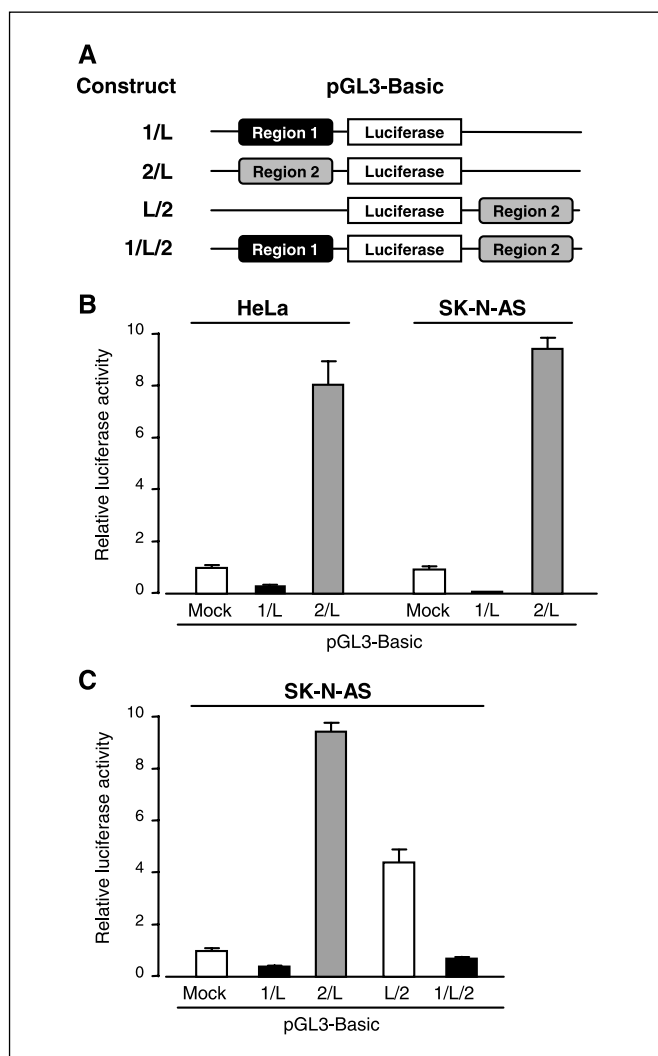


Figure 2. Promoter activity of the CpG island of *NR112*. pGL3-Basic vector, each containing a 1,060 bp 5' fragment (region 1) or a 480 bp CpG island (region 2) of *NR112* in front of and/or downstream of the luciferase gene (1/L, 2/L, L/2, and 1/L/2; A), or pGL3-Basic empty vector (mock), was transfected into HeLa or SK-N-AS cells to evaluate promoter activity of region 1 and region 2 (B) and enhancer activity of region 2 (C). Luciferase activities were normalized versus an internal control. Columns, means of three separate experiments, each done in triplicate; bars, SE.

containing region 1 in front of the luciferase reporter gene and region 2 downstream of the luciferase gene (Fig. 2A, 1/L/2). Although region 2 downstream of the luciferase gene (Fig. 2A, L/2) showed some promoter activity, region 2 revealed no enhancer activity for region 1 (Fig. 2C).

Analysis of *NR112* methylation and expression in primary neuroblastoma tumors. We next examined methylation status of the *NR112* CpG island in 51 surgically resected primary neuroblastomas using COBRA (Table 2). Clearly methylated alleles were detected in nine of the tumors (17%; Fig. 3A). The appearance of partial methylation observed in those nine tumors can be explained by the unavoidable contamination of non-tumorous cells in the specimens. Five of the nine tumors (55%) had undergone *MYCN* amplification, whereas only 3 of 42 (7%) unmethylated tumors showed amplification of *MYCN* (Table 2). Moreover, methylation of region 2 of the *NR112* gene was more

frequently detected in advanced tumors (stages III and IVa; $P = 0.0234$, Fisher's exact test), tumors from patients with poor outcome (dead from disease; $P = 0.0135$, Fisher's exact test), and tumors from patients >1 year old ($P = 0.052$, Fisher's exact test), although the difference did not quite reach statistical significance in terms of patient age. In the 47 neuroblastoma cases where high-quality RNAs were available for expression analysis, a clear correlation between the methylation status of the CpG island and expression level of *NR112* mRNA was observed (Fig. 3B and C). By means of real-time quantitative RT-PCR experiments, we saw a statistically significant inverse correlation between expression of *NR112* mRNA and tumor stage ($P = 0.0137$, Mann-Whitney U test) or *MYCN* amplification ($P = 0.0003$, Mann-Whitney U test; Fig. 3C).

Suppression of cell growth after restoration of *NR112* expression. To gain further insight into the potential role of *NR112* in neuroblastoma carcinogenesis, we investigated whether restoration of *NR112* expression would suppress growth of neuroblastoma cells lacking endogenous *NR112* expression using two *NR112* expression constructs, a Myc-tagged full coding sequence of *NR112* alone (pCMV-Tag3-*NR112*) and one fused to the constitutively active herpes virus VP-16 transactivation domain (pCMV-Tag3-VP-*NR112*). The VP-16-*NR112* chimeric protein showed stronger transactivating activity than *NR112* alone in a reporter assay using a reporter construct containing *NR112* response elements from the *CYP3A4* promoter (data not shown). After selecting drug-resistant colonies in transient transfection experiments, we found that colonies of *NR112*-transfected cells were remarkably fewer than in cultures of control transfectants and the effect of VP-16-*NR112* was much greater than that of *NR112* (Fig. 4A). Furthermore, VP-16-*NR112* stable transfectants

Table 2. Correlation between patient profiles and *NR112* methylation status in 51 cases with neuroblastoma

Characteristics	Cases n	COBRA on <i>NR112</i> region 2*		
		Negative n	Positive n	P^\dagger
Total	51	42	9	
Age (y)				
<1	33	30	3	0.052
≥ 1	18	12	6	
Stage [‡]				
I, II, IVS	30	23	2	0.0234
III, IVa	21	16	7	
<i>MYCN</i>				
Nonamplified	43	39	4	0.024
Amplified	8	3	5	
Outcome				
Alive	44	39	5	0.0135
Dead	7	3	4	

NOTE: Statistically significant values are in boldface.

*COBRA was done as described in Materials and Methods.

[†] P values are from Fisher's exact test and were statistically significant when <0.05.

[‡]Tumor stage was classified according to the International Neuroblastoma Staging System.

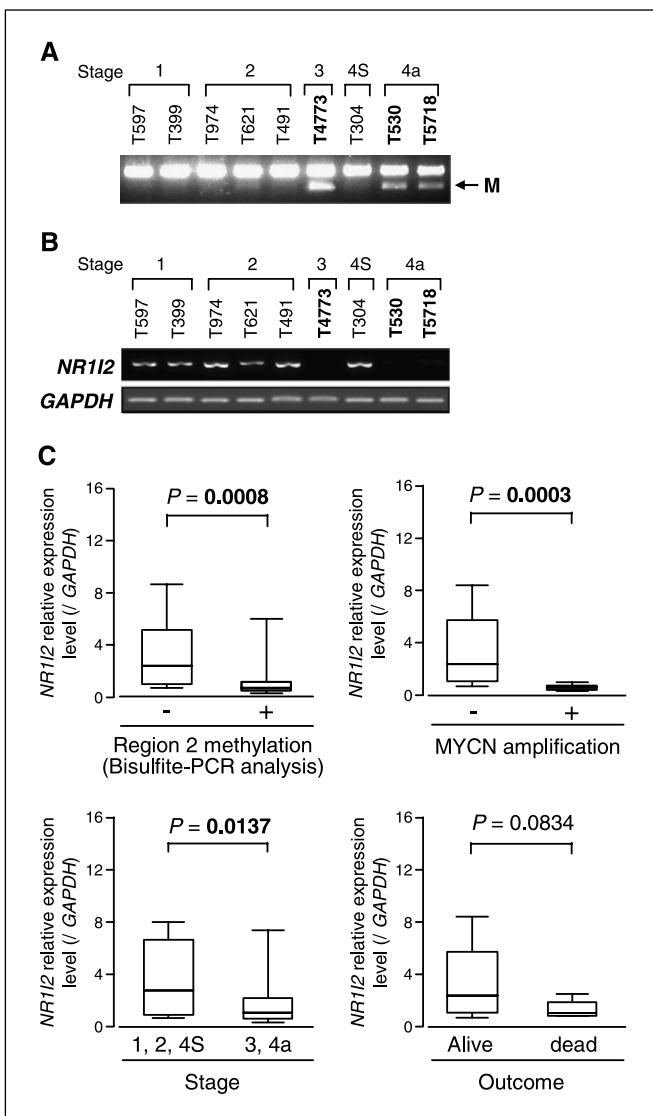


Figure 3. Methylation status and expression levels of *NR1I2* in primary neuroblastoma tumors. *A*, representative results of COBRA of the *NR1I2* CpG island (region 2). *M*, methylated alleles restricted by *HhaI*. *B*, representative results of RT-PCR analysis of *NR1I2* mRNA expression. *GAPDH* was used as an internal control. Note that tumors showing methylation in Fig. 2*A* (T4773, T530, and T5718) showed decreased expression of *NR1I2*. *C*, expression of *NR1I2* mRNA in primary neuroblastoma tumors, compared with methylation status of the CpG island of *NR1I2* region 2, *MYCN* amplification status, tumor stage, and patient outcomes. The levels of *NR1I2* mRNA expression were determined by real-time quantitative RT-PCR experiments. Significantly higher expression of *NR1I2* was observed in tumors without methylation of the CpG island ($P = 0.0008$, Mann-Whitney *U* test), in stage I, II, and IVS tumors ($P = 0.0137$, Mann-Whitney *U* test), and in *MYCN*-nonamplified tumors ($P = 0.0003$, Mann-Whitney *U* test) compared with tumors with methylation of the CpG island, stage III or IVa tumors, and *MYCN*-amplified tumors. Higher expression of *NR1I2* was also observed in living, disease-free patients compared with those who had died of their tumors, although the difference did not reach statistical significance ($P = 0.0834$, Mann-Whitney *U* test).

established from a cell line (SMS-KAN) without endogenous expression of this gene showed a lower growth rate than control vector-transfected cells regardless of VP-16-NR1I2 expression level (Fig. 4*B* and *C*). The same result was obtained in other cell line (data not shown).

Screening of possible target genes for NR1I2. To identify possible transcriptional targets for NR1I2, we did expression

array analysis in an independent VP-16-NR1I2 stable transfectant established from SMS-KAN, in a comparison with vector-transfected cells. We twice obtained independent experimental data (first, Cy3-B1/Cy5-vector; second, Cy5-B1/Cy3-vector) and compiled a list of 105 genes that showed ratios >1.5 in both experiments (Supplementary Table S1). Semiquantitative RT-PCR analysis revealed up-regulation of *CYP3A4*, a known transcriptional target of *NR1I2*, in VP-16-NR1I2 stable transfectant, indicating the reliability of our system for detecting target genes (Supplementary Fig. S1). To validate the expression array data, we did semiquantitative RT-PCR analyses of 10 other genes (Fig. 4*D*), which have been previously reported as tumor-associated genes, using two independent VP-16-NR1I2 stable transfectants established from SMS-KAN cells (KAN-B1 and KAN-B2) and one stable transfectant from GOTO cells (GOTO-A1). GOTO-A1 also showed a lower growth rate than control vector-transfected cells (data not shown). The RT-PCR results for KAN-B1 confirmed up-regulation of seven genes except for *BARD1*, *EXT1*, and *MCM5* (Fig. 4*D*). Notably, only *PLA2G2A* showed increased expression in all stable transfectants examined compared with their control cells (Fig. 4*D*; Supplementary Fig. S1).

Discussion

In the study presented here, we identified a novel target for CpG island methylation, *NR1I2*, observed mainly in advanced neuroblastomas, through a genome-wide exploration of highly methylated DNA fragments using BAMCA. A clear inverse correlation emerged between CpG island methylation and the expression status of *NR1I2* both in cell lines and primary tumors of neuroblastoma (i.e., hypermethylation and silencing of *NR1I2* were more frequent in advanced neuroblastoma tumors). Together with a shown growth suppressive effect of exogenous NR1I2, the data suggested that *NR1I2* was likely to be a tumor suppressor gene associated with clinical and/or biological aggressiveness of neuroblastoma. Our results further underscored the promise of BAMCA as a high-throughput screening method for methylated sites in cancer genomes on an array platform.

BAMCA, however, has some disadvantages: (a) It examines only a limited number of CpG sites within a CpG island because only *SmaI/XmaI* sites are used to search differentially methylated CpGs. (b) It identifies BACs, which contain differentially methylated sequences between test and reference DNAs, although sequences are not always associated with promoter regions of genes. (c) It misses differentially methylated sequences/genes without BACs spotted on the BAC array used. To improve the sensitivity of array-based methylation screening, it is possible to use other methylation-sensitive restriction sites as indicators, including *NotI* site (20). However, BAMCA may quickly provide the list of possible target genes for methylation within identified BAC clones using information from human genome database without cloning and sequencing of enriched fragments, suggesting that it may have important applications in population-based studies of CpG island methylation.

NR1I2 locates at 3q13.33, a chromosomal region that is not often involved in loss of heterozygosity or copy number losses in neuroblastoma (21, 22). Indeed, most of the cell lines we used in this study showed normal copy number in 3q (13), suggesting that a homozygous inactivation of *NR1I2* might occur by biallelic

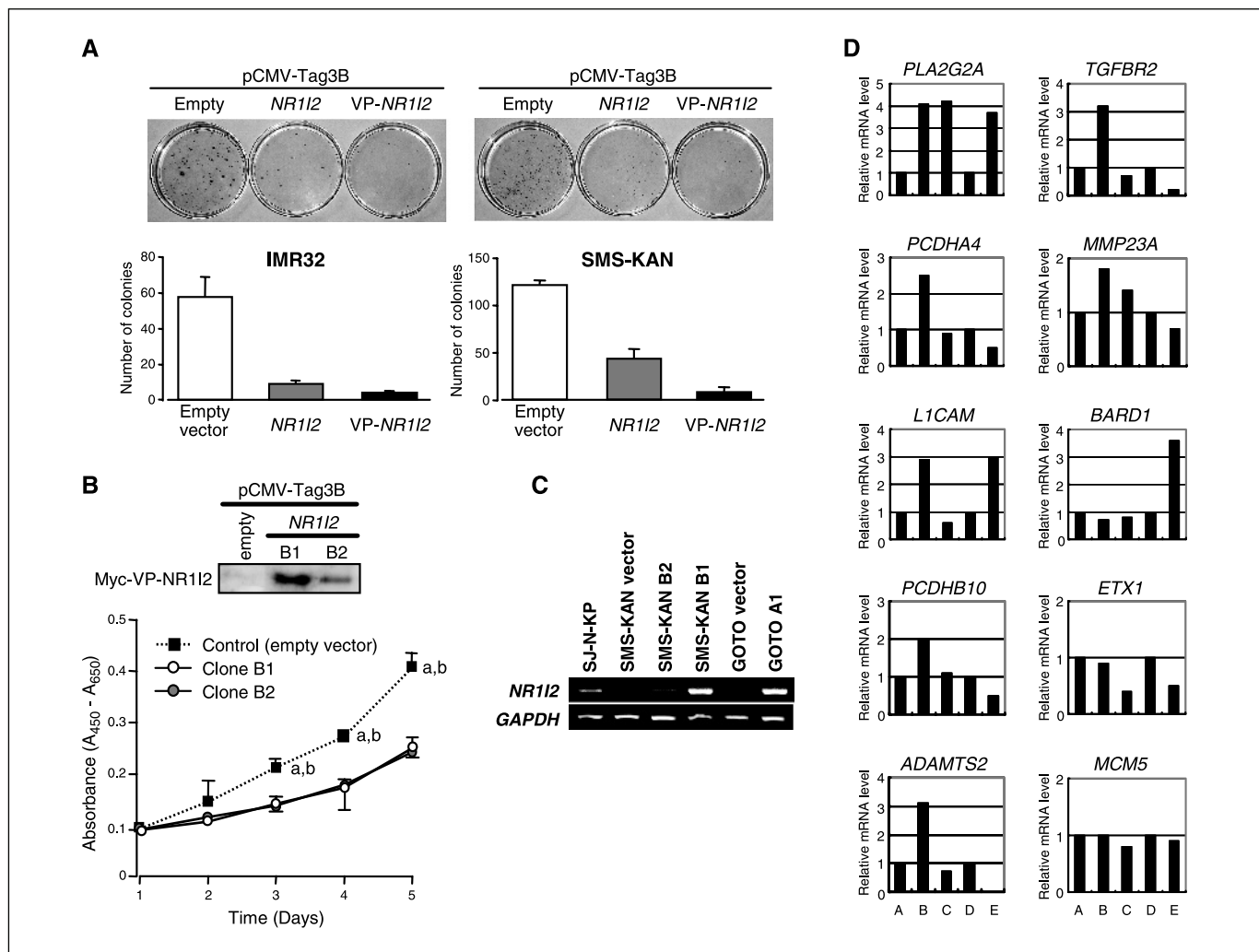


Figure 4. Effect of restoration of NR112 expression on growth of neuroblastoma cells. *A*, top, colony formation assays using neuroblastoma cell lines. Cells without NR112 expression (IMR32 and SMS-KAN) were transfected with Myc-tagged construct containing NR112 (pCMV-Tag3B-NR112), VP-NR112 (pCMV-Tag3B-VP-NR112), or empty vector (pCMV-Tag3B), and selected for 3 weeks with G418. Bottom, quantitative analysis. Columns, mean of three separate experiments, each done in triplicate; bars, SE. *B*, inhibitory effect of stably transfected NR112 on the growth of SMS-KAN cells transfected with pCMV-Tag3B-VP-NR112 or empty vector and selected with G418 to establish clones stably expressing NR112. Top, two clones transfected with pCMV-Tag3B-VP-NR112 (B1 and B2) were subjected to Western blot analysis using 10 μ g of protein extract and anti-Myc-Tag antibody. Both expressed Myc-tagged VP-NR112 protein. Bottom, effect of stable NR112 expression on the growth of SMS-KAN cells. Cell viability was determined by water-soluble tetrazolium salt assay at the indicated times. Points, means of three separate experiments; bars, SE. Statistical analysis used the Mann-Whitney *U* test: a, control versus clone B1; b, control versus clone B2. All *P* < 0.05. *C*, the mRNA expression level of NR112 in endogenously NR112-positive cells (SK-N-KP) as well as stably transfected cells (SMS-KAN-B1, SMS-KAN-B2, and GOTO-A1) and their mock-transfected control (KAN-vector and GOTO-vector). *D*, confirmation of microarray results by semiquantitative RT-PCR of possible target genes using two stable transfectants established from SMS-KAN (KAN-B1 and KAN-B2) and one transfectant from GOTO (GOTO-A1) with their mock-transfected control cells A, SMS-KAN mock-control; B, KAN-B1; C, KAN-B2; D, GOTO mock-control; E, GOTO-A1. PCR products were electrophoresed in 3% agarose gel and band quantification was done with LAS-3000 (Fujifilm, Tokyo, Japan). After normalization with GAPDH, expression level of each gene in each transfectant relative to its corresponding mock-transfected control was recorded as a fold increase in relative expression level. Primer sequences and cycling numbers for PCR of each gene are available on request.

methylation. Similar findings have been reported for several genes, such as *RASSF1* (3p21.3), *DAPK* (9q34.1), and *THBS1* (15q15), which are located in regions not frequently deleted, although some methylated genes, such as *ARF* and *INK4A* (9p21), and *CASP8* (2q23), are in fact on regions frequently deleted in neuroblastoma (23). Therefore, both biallelic methylation and monoallelic methylation with allele loss may be important mechanisms for inactivating tumor-associated genes in this disease.

Our promoter assays showed that CpG island around exon 3 (region 2) shows promoter activity, but CpG-rich 5' region containing exon 1 and its 5' upstream sequences (region 1) does

not. Region 2 shows no enhancer activity for region 1 (Fig. 2). The methylation status of region 2, but not region 1, was highly and inversely correlated with the expression of NR112, especially the most major variant of NR112, variant 1, starting from exon 1a. Those results suggest that the methylation status of CpG residues in region 2 might be responsible for the silencing of this gene and contributed to loss of function of NR112 protein in neuroblastoma. A few studies, including ours, have shown that promoter activity can occur in fragments, especially CpG islands, not containing transcriptional starting sites (17, 24, 25). It is possible that methylation that occurred in those CpG islands with promoter activity may silence gene expression from specific starting sites.

Among numerous hypermethylated genes reported in neuroblastoma (3–8), *CASP8* seems to be inactivated through promoter methylation in advanced neuroblastoma tumors where *MYCN* is amplified (4). Those findings, along with ours, suggest that (a) unknown mechanisms contribute to progression of neuroblastoma by causing genetic alterations, including *MYCN* amplification, as well as methylation-mediated inactivation of a subset of tumor suppressor genes; (b) methylation-mediated inactivation of a subset of tumor suppressor genes may cause genetic changes that lead to progression of neuroblastoma; or (c) *MYCN* amplification and/or other alterations in advanced neuroblastomas may bring about a CpG island methylator phenotype (3). Gonzalez-Gomez et al. (23) reported that higher aggressiveness, represented at the molecular level by concurrent *MYCN* amplification and 1p loss in neuroblastoma, was not paralleled by an accumulation of methylation events among various genes they examined, suggesting that CpG island methylation in advanced neuroblastoma could be specific to a subset of genes.

The *NR1I2* gene encodes an orphan nuclear receptor that plays a key role in the regulation of xenobiotic response by controlling expression of drug metabolizing and clearance molecules (26–28). NR1I2 protein activates expression of genes encoding proteins such as CYP3A4 and ABCB1, which reduce the concentrations of xenochemicals and toxic bile acids (29). However, effects of NR1I2 on cell growth or expression of growth-regulating genes have never been clarified, although we have shown here that the induction of ectopic NR1I2 inhibited growth of neuroblastoma cells. Other nonsteroidal nuclear receptors, such as all-*trans* retinoic acid receptor and vitamin D₃ receptor, which form heterodimers with the 9-*cis* retinoic acid receptor in the same way as NR1I2, mediate antiproliferative and differentiation-promoting activities toward several malignant cell types (30, 31). Therefore, growth-suppressive activity might be one of the normal functions of NR1I2 although its mechanisms remain unknown.

To achieve some clarity with respect to the growth inhibitory activity of NR1I2, we tried to determine its putative transcriptional targets. Among 105 genes through an expression array analysis, we selected 10 genes for validation by semiquantitative PCR based on their possible cancer-associated function (Online Mendelian Inheritance in Man),⁸ and identified one candidate, *PLA2G2A*, encodes secretory phospholipase A2, as a possible target of NR1I2, although it will be needed to determine whether *PLA2G2A* is a direct or indirect target. This product qualifies as a tumor suppressor because mice lacking *PLA2G2A* expression show increased colonic polyposis (32). Interestingly, *PLA2G2A* was mapped to chromosome 1p36, a region frequently implicated in the pathogenesis of neuroblastoma (33). Further screening of possible targets of NR1I2 will be necessary to clarify how NR1I2 regulates neuroblastoma cell growth.

Because only 7 of 51 neuroblastoma patients in our study died during follow-up periods, we did not perform a survival analysis. However, the high prevalence of *NR1I2* silencing through DNA methylation that we observed in aggressive neuroblastomas, along with the shown growth suppression activity of NR1I2, indicate that this molecule might serve as a diagnostic marker to predict prognosis.

Acknowledgments

Received 3/30/2005; revised 9/2/2005; accepted 9/13/2005.

Grant support: Grants-in-Aid for Scientific Research on Priority Areas (C) from the Ministry of Education, Culture, Sports, Science, and Technology, Japan; a Grant-in-Aid from Core Research for Evolutionary Science and Technology of Japan Science and Technology; Center of Excellence program for Frontier Research on Molecular Destruction and Reconstitution of Tooth and Bone; program for promotion of Fundamental Studies in Health Sciences of the Pharmaceuticals and Medical Devices Agency; and Third Term Comprehensive Control Research for Cancer of the Ministry of Health, Labour, and Welfare.

The costs of publication of this article were defrayed in part by the payment of page charges. This article must therefore be hereby marked *advertisement* in accordance with 18 U.S.C. Section 1734 solely to indicate this fact.

We thank Ai Watanabe and Ayako Takahashi for technical assistance.

⁸ <http://www.ncbi.nlm.nih.gov/Omim/omimhelp.html>.

References

- Brodeur GM. Neuroblastoma: biological insights into a clinical enigma. *Nat Rev Cancer* 2003;3:203–16.
- Westermann F, Schwab M. Genetic parameters of neuroblastomas. *Cancer Lett* 2002;184:127–47.
- Abe M, Ohira M, Kaneda A, et al. CpG island methylator phenotype is a strong determinant of poor prognosis in neuroblastomas. *Cancer Res* 2005;65:828–34.
- Teitz T, Wei T, Valentine MB, et al. Caspase 8 is deleted or silenced preferentially in childhood neuroblastomas with amplification of MYCN. *Nat Med* 2000;6:529–35.
- Astuti D, Agathangelou A, Honorio S, et al. RASSF1A promoter region CpG island hypermethylation in pheochromocytomas and neuroblastoma tumours. *Oncogene* 2001;20:7573–7.
- Yan P, Muhlethaler A, Bourloulou KB, Beck MN, Gross N. Hypermethylation-mediated regulation of CD44 gene expression in human neuroblastoma. *Genes Chromosomes Cancer* 2003;36:129–38.
- Yang Q, Liu S, Tian Y, et al. Methylation-associated silencing of the thrombospondin-1 gene in human neuroblastoma. *Cancer Res* 2003;63:6299–310.
- Yang Q, Liu S, Tian Y, et al. Methylation-associated silencing of the heat shock protein 47 gene in human neuroblastoma. *Cancer Res* 2004;64:4531–8.
- Baylin SB, Herman JG, Graff JR, Vertino PM, Issa JP. Alterations in DNA methylation: a fundamental aspect of neoplasia. *Adv Cancer Res* 1998;72:141–96.
- Ushijima T. Detection and interpretation of altered methylation patterns in cancer cells. *Nat Rev Cancer* 2005;5:223–31.
- Toyota M, Ho C, Ahuja N, et al. Identification of differentially methylated sequences in colorectal cancer by methylated CpG island amplification. *Cancer Res* 1999;59:2307–12.
- Inazawa J, Inoue J, Imoto I. Comparative genomic hybridization (CGH)-arrays pave the way for identification of novel cancer-related genes. *Cancer Sci* 2004;95:559–63.
- Saito-Ohara F, Imoto I, Inoue J, et al. PPM1D is a potential target for 17q gain in neuroblastoma. *Cancer Res* 2003;63:1876–83.
- Brodeur GM, Pritchard J, Berthold F, et al. Revision of the international criteria for neuroblastoma diagnosis, staging, and response to treatment. *J Clin Oncol* 1993;11:1466–77.
- Matsumura T, Michon J. Treatment of localized neuroblastoma. In: Brodeur GM, Sawada T, Tsuchida Y, Voute PA, editors. *Neuroblastoma*. Amsterdam (the Netherlands): Elsevier Science BV; 2000. p. 403–16.
- Tsuchida Y, Kaneko M. Treatment of advanced neuroblastoma: the Japanese experience. In: Brodeur GM, Sawada T, Tsuchida Y, Voute PA, editors. *Neuroblastoma*. Amsterdam (the Netherlands): Elsevier Science BV; 2000. p. 453–70.
- Sonoda I, Imoto I, Inoue J, et al. Frequent silencing of low density lipoprotein receptor-related protein 1B (LRP1B) expression by genetic and epigenetic mechanisms in esophageal squamous cell carcinoma. *Cancer Res* 2004;64:3741–7.
- Inoue J, Otsuki T, Hirasawa A, et al. Overexpression of PDZK1 within the 1q12-q22 amplicon is likely to be associated with drug-resistance phenotype in multiple myeloma. *Am J Pathol* 2004;165:71–81.
- Lamba V, Yasuda K, Lamba JK, et al. PXR (NR1I2): splice variants in human tissues, including brain, and identification of neurosteroids and nicotine as PXR activators. *Toxicol Appl Pharmacol* 2004;199:251–65.
- Ching TT, Maunakea AK, Jun P, et al. Epigenome analyses using BAC microarrays identify evolutionary conservation of tissue-specific methylation of *SHANK3*. *Nat Genet* 2005;37:645–51.
- Brinkschmidt C, Christiansen H, Terpe HJ, et al. Comparative genomic hybridization (CGH) analysis of neuroblastomas—an important methodological approach in paediatric tumour pathology. *J Pathol* 1997;181:394–400.
- Takita J, Hayashi Y, Yokota J. Loss of heterozygosity in neuroblastomas—an overview. *Eur J Cancer* 1997;33:1971–3.
- Gonzalez-Gomez P, Bello MJ, Lomas J, et al. Aberrant methylation of multiple genes in neuroblastic tumours. Relationship with MYCN amplification and allelic status at 1p. *Eur J Cancer* 2003;39:1478–85.
- Kolb A. The first intron of the murine β -casein gene contains a functional promoter. *Biochem Biophys Res Commun* 2003;306:1099–105.

25. Nakagawachi T, Soejima H, Urano T, et al. Silencing effect of CpG island hypermethylation and histone modifications on *O*6-methylguanine-DNA methyltransferase (MGMT) gene expression in human cancer. *Oncogene* 2003;22:8835-44.
26. Blumberg B, Sabbagh W, Juguilon H, et al. SXR, a novel steroid and xenobiotic-sensing nuclear receptor. *Genes Dev* 1998;12:3195-205.
27. Kliewer SA, Moore JT, Wade L, et al. An orphan nuclear receptor activated by pregnanes defines a novel steroid signaling pathway. *Cell* 1998;92:73-82.
28. Xie W, Barwick JL, Downes M, et al. Humanized xenobiotic response in mice expressing nuclear receptor SXR. *Nature* 2000;406:435-9.
29. Synold TW, Dussault I, Forman BM. The orphan nuclear SXR coordinately regulates drug metabolism and efflux. *Nat Med* 2001;7:584-90.
30. Altucci L, Gronemeyer H. Nuclear receptors in cell life and death. *Trends Endocrinol Metab* 2001;12:460-8.
31. Rao A, Coan A, Welsh JE, Barclay WW, Koumenis C, Cramer SD. Vitamin D receptor and p21/WAF1 are targets of genistein and 1,25-dihydroxyvitamin D₃ in human prostate cancer cells. *Cancer Res* 2004;64:2143-7.
32. Haluska FG, Thiele C, Goldstein A, Tsao H, Benoit EP, Housman D. Lack of phospholipase A2 mutations in neuroblastoma, melanoma and colon-cancer cell lines. *Int J Cancer* 1997;72:337-9.
33. Praml C, Savelyeva L, Le Paslier D, et al. Human homologue of a candidate for the *Mom1* locus, the secretory type II phospholipase A2 (PLA2S-II), maps to 1p35-36.1/D1S199. *Cancer Res* 1995;55:5504-6.

Cancer Research

The Journal of Cancer Research (1916–1930) | The American Journal of Cancer (1931–1940)

Methylation-Associated Silencing of the *Nuclear Receptor 1/2* Gene in Advanced-Type Neuroblastomas, Identified by Bacterial Artificial Chromosome Array-Based Methylated CpG Island Amplification

Akiko Misawa, Jun Inoue, Yuriko Sugino, et al.

Cancer Res 2005;65:10233-10242.

Updated version Access the most recent version of this article at:
<http://cancerres.aacrjournals.org/content/65/22/10233>

Supplementary Material Access the most recent supplemental material at:
<http://cancerres.aacrjournals.org/content/suppl/2006/01/31/65.22.10233.DC1>

Cited articles This article cites 29 articles, 10 of which you can access for free at:
<http://cancerres.aacrjournals.org/content/65/22/10233.full#ref-list-1>

Citing articles This article has been cited by 5 HighWire-hosted articles. Access the articles at:
<http://cancerres.aacrjournals.org/content/65/22/10233.full#related-urls>

E-mail alerts [Sign up to receive free email-alerts](#) related to this article or journal.

Reprints and Subscriptions To order reprints of this article or to subscribe to the journal, contact the AACR Publications Department at pubs@aacr.org.

Permissions To request permission to re-use all or part of this article, use this link
<http://cancerres.aacrjournals.org/content/65/22/10233>.
Click on "Request Permissions" which will take you to the Copyright Clearance Center's (CCC) Rightslink site.